Advances in Concrete Construction, *Vol. 6, No. 5 (2018) 527-543*
DOI: https://doi.org/10.12989/acc.2018.6.5.527

Crack control of precast deck loop joint using high strength concrete

Changsu Shim[a], Chi dong Lee[*] and Sung-woong Ji[b]

Department of Civil Engineering, College of Engineering, Chung-Ang University, 84 Heukseok-ro, Dongjak-gu, Seoul 156-756, Republic of Korea

(Received February 27, 2018, Revised October 25, 2018, Accepted October 26, 2018)

Abstract. Crack control of precast members is crucial for durability. However, there is no clear provision to check the crack width of precast joints. This study presents an experimental investigation of loop joint details for use in a precast bridge deck system. High strength concrete of 130 MPa was chosen for durability and closer joint spacing. Static tests were conducted to investigate the cracking and ultimate behavior of test specimens. The experimental results indicate that current design codes provide reasonable estimation of the flexural strength and cracking load of precast elements with loop joint of high strength concrete. However, the crack width control of the loop joints with high strength concrete by the current design practices was not appropriate. Some recommendations to improve crack control of the loop joint were derived.

Keywords: loop joint; cracking; precast deck; high strength concrete; static test

1. Introduction

Current transportation infrastructures are aging and need strengthening or replacement. Many of the bridges in the transportation network are approaching or have passed their service lives. The part of a bridge most affected by aging is the deck slab, because this slab is directly exposed to traffic loading and corrosion caused by de-icing salts (Lewis 2009, Shim *et al.* 2010). In this case, replacement of the deteriorated parts of the bridge structure with full depth precast slabs is one of the leading solutions to the problem. Moreover, this solution is receiving significant attention to eradicate the aging problem of bridge structures. The precast structure helps to reduce construction cost and time, improves constructability, and ensures quality control. In spite of the beneficial effects, serviceability and durability problems, such as cracking and corrosion of steel by water leakage at the connection parts, have been reported by many researchers (Issa *et al.* 1995).

Durability is one of the main issues among the different limit state design criteria. Nowadays, there is a growing demand for durable prefabricated structural systems that can facilitate accelerated on-site construction in order to minimize its impact on the environment. Precast members can provide higher quality, with accelerated and safer construction; however, expansion

∗Corresponding author, Ph.D. Candidate, E-mail: doinda@hanmail.net
[a]Professor, E-mail: csshim@cau.ac.kr
[b]Researcher, E-mail: woong0327@cau.ac.kr

http://www.techno-press.org/?journal=acc&subpage=7 ISSN: 2287-5301 (Print), 2287-531X (Online)

of offsite prefabrication of precast elements requires increased reliance on the long-term performance of the cast-in-place concrete connections between these components. The cast-in-place joints have often showed inadequate performance that resulted in additional cost for repairs.

For accelerated replacement of decks, the precast panel system has received notable attention. This system is used in several countries because it can guarantee higher quality and minimize formworks (Shim *et al.* 2010). Post-tensioning is used across the joint to provide structurally monolithic behavior and to ensure that the joint remains intact. However, the use of post-tensioning makes the design more complicated, and future partial replacement of the precast decks becomes another concern.

Extensive research on various types of precast joints has already been performed (Shim *et al.* 2000, Issa *et al.* 1995, Ryu *et al.* 2007). The ultimate behavior of the precast deck with loop joints was similar to that of ordinary RC members without joints. Considering the previous studies, the loop joint spacing was designed to satisfy the current requirements of development length (Shim *et al.* 2000, Issa *et al.* 1995, Ryu *et al.* 2007). The study on the load carrying capacities of loop joints subjected to combined tension and bending has also been performed (Jeorgensen *et al*. 2015). Recently, ultra-high performance concrete (UHPC) was introduced to improve the practicality of precast decks (Perry and Royce 2007). The UHPC joint has improved the continuity and reduced the joint size and complexity of additional post-tensioning processes. UHPC joints represent an alternative which can satisfy the requirements on mechanical properties of joints, on construction and economy (Vitek *et al.* 2016).

Many researchers have already performed studies on the factors that influence the crack width, such as reinforcement ratio and diameter, joint spacing, and strength of concrete. The influence of the reinforcement ratio in the calculation of crack width is substantial, whereas the influence of the strength of concrete is less important (Creazza and Russo 1999). In the case of a precast deck with loop joints, the crack width is mainly influenced by the diameter of rebars (Ryu *et al.* 2007).

Current design codes, such as AASHTO LRFD, ACI 318, and Eurocode-2, specify that the crack width can be controlled by considering design parameters such as stress in tension reinforcement, diameter of rebar, spacing, and cover depth. The crack width criterion based on the theory of Eurocode-2 uses the strains of steel and concrete as main variables, and it also considers the direction of the main reinforcement. It is further adjusted by using empirical coefficients. The criteria of crack control mentioned in the AASHTO LRFD and ACI 318 specifications are based on empirical experiments. Additionally, the specifications for high strength concrete are not provided in the design codes. In order to allow the use of a high performance material for the joint fill, it is necessary to provide reliable evidence on its strength, crack width, and durability.

In this work, an experimental study was performed to investigate the cracking behavior at the joint part of precast members. High strength concrete was used as joint fill material, and various joint details were chosen to investigate the appropriate approaches to control cracking. Different surface conditions of the precast loop joint were also considered to suggest proper quality control of the joint. The structural performance of the joints was evaluated in terms of cracking load, crack width, and flexural strength.

2. Experimental program

The main purpose of this experimental program was to evaluate the flexural behavior of the precast deck with loop joints in which high strength concrete was filled. Cracking and crack width

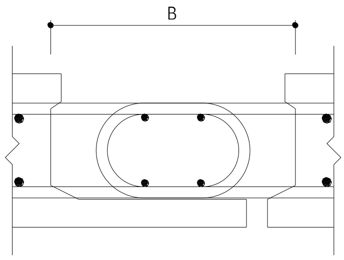

Fig. 1 Details of joint

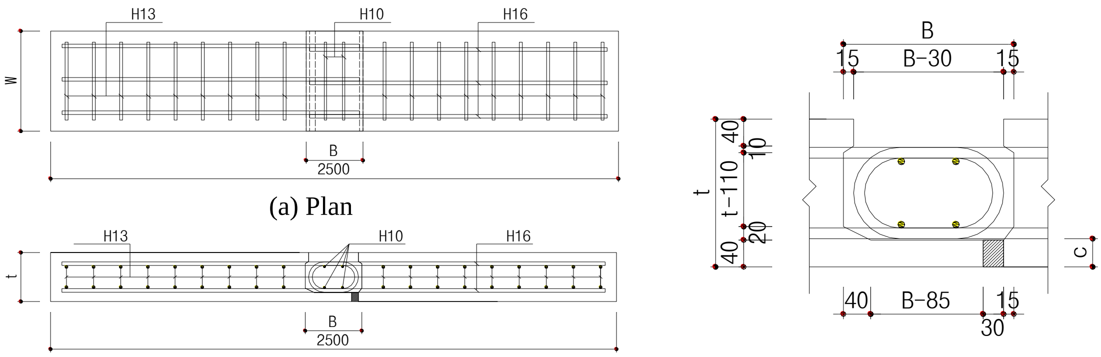

(a) Plan

(b) Elevation

(c) Joint detail

Fig. 2 Schematic diagrams of designed specimens

according to the stress level of the tensile reinforcements were the main interest in the test.

2.1 Details of test specimens

A U-bar joint detail was designed for full-depth precast decks to eliminate the formwork, as illustrated in Fig. 1. Nine specimens with length of 2.5 m were designed and fabricated, as summarized in Table 1. The section dimensions of 300 mm width and 220 mm depth were chosen for the DD250-16 – DD350-19 specimens. Moreover, the width of 400 mm and depth of 300 mm were chosen for the DD300-22S – DD300-22B specimens. It was anticipated that the joint spacing would be a crucial factor to ensure the development length for the reinforcement anchorage.

Each specimen comprised two segments and a joint part that includes three layers of loop bars, and was filled with cast-in-place concrete. The specimens were fabricated according to the current practices of precast segments on both sides and in-situ casting joints. To minimize the formwork, specific shapes of the joint detail, such as that in Fig. 1, were devised by using projected concrete parts. Watertight rubber was installed between the two segments, as shown in Fig. 2(c). Longitudinal reinforcement of 16 mm, 19 mm, and 22 mm, and transverse reinforcement of 10 mm was used in all the specimens.

To develop compression and tension in the reinforcement, the criterion of development length is provided in ACI 318 (2014). The criterion of development length for hooks is used for the design of the loop joint details. The calculation of hook development length directly depends on the diameter of the reinforcement. The high-strength concrete of 130 MPa is out of the scope of the provision.

Table 1 Main variables of test specimens

Specimen	Diameter of loop bar (mm) / Yield stress (MPa)	Joint Spacing *B* (mm)	Slab Width *W* (mm)	Slab Thickness *t* (mm)	Concrete Cover *c* (mm)	Steel ratio ρ	Joint fill Compressive strength (MPa)
DD250-16	16 / 400	250	450	220	42	0.779	130
DD250-19	19 / 400	250	450	220	40.5	1.124	130
DD300-16	16 / 400	300	450	220	42	0.779	130
DD300-19	19 / 400	300	450	220	40.5	1.124	130
DD350-16	16 / 400	350	450	220	42	0.779	130
DD350-19	19 / 400	350	450	220	40.5	1.124	130
DD300-22S	22 / 400	300	400	300	29	0.744	40
DD300-22C	22/ 400	300	400	300	29	0.744	40
DD300-22B	22 / 400	300	400	300	29	0.744	40

S: steel brushing; C: chipping; B: bond adhesive coating

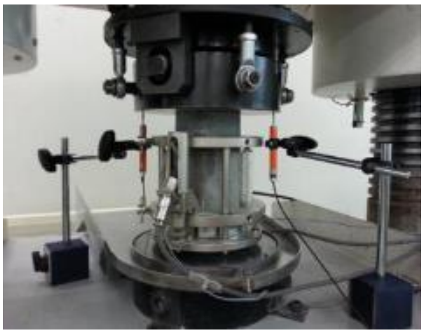

Fig. 3 ASTM methods to measure concrete properties

Table 2 Mechanical properties of high strength concrete

Properties	Testing method	Results (MPa)	Remarks
Compressive strength	ASTM C 109 (modified)	130	28 day min. strength
Elastic modulus	ASTM C 469	43,000	28 day
Flexural strength	ASTM C 1609	9.4	-

2.2 Material properties

In this experimental program, it was planned to use two types of concrete for joint fill; one is normal concrete with design compressive strength of 40 MPa and the other one is high strength concrete with design compressive strength of 130 MPa. The properties of the high strength concrete poured in the joint parts were examined by ASTM testing methods as shown in Fig. 3 and are summarized in Table 2.

Table 2 presents the results of mechanical properties of the high strength concrete, while Table 3 summarizes the concrete compressive strength test results according to the curing days. The cylinder specimen is 100 mm in diameter and 200 mm in height. The strength values are the average values of the three specimens of each type. The compressive strength of concrete for

Table 3 Results of cylinder concrete compressive strength tests

Curing days	Concrete compressive strength (MPa)			
	Precast member		Joint fill	
	High-strength	Normal-strength	High-strength	Normal-strength
3	38	28	-	19
7	47	34	136	25
12	51	-	-	-
28	53	51	-	51

Fig. 4 Casting of high strength concrete in a joint

precast members was 50 MPa. Yield strength of the deformed rebar with diameters of 16 mm, 19 mm, and 22 mm was 400 MPa.

2.3 Fabrication of the specimens

The test specimens for this experimental program were fabricated by the following procedure. Firstly, precast segments were manufactured, as designed, by using an ordinary concrete in a factory. Subsequent to the form removal of the precast segments, the joint part interfaces were cleaned. They were handled by performing steel brushing as one of the surface treatments for the specimens with high strength fill. Then, to measure the strains of reinforcement, strain gauges, which should be embedded in the concrete parts, were attached to the steel reinforcement prior to casting the joints. Fig. 4 shows the last step when the high strength concrete was poured into the joint parts with the overlapping loop bars connecting the two precast segments.

Various influencing factors, such as externally imposed loads, drying shrinkage, and ambient temperature changes, cause that the tensile stress exceeds the tensile strength of the joint interface, which results in cracking. The cast-in-place concrete joint must not interfere with the flexural and shear continuity through the interface between the precast concrete and the concrete that is placed thereafter. To achieve this continuity, the hardened concrete must be clean and free of laitance. Therefore, steel brushing was applied to all the specimens. Chipping or coating of bond adhesives were conducted for the specimens of normal strength fill (DD300-22C and DD300-22B). It helped to improve the bond strength of the interface.

2.4 Measurement plan and loading

Three-point loading static tests were performed to investigate the flexural strength and cracking

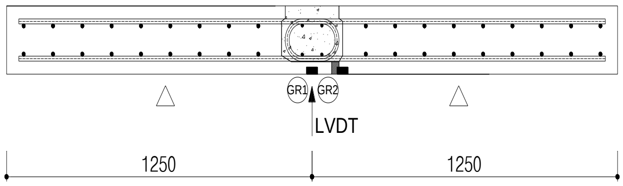

(a) LVDT and Omega gauges

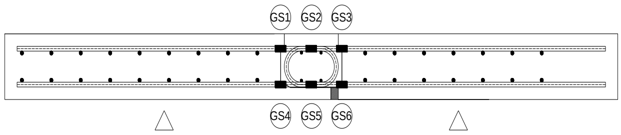

(b) Steel strain gauges (Elevation)

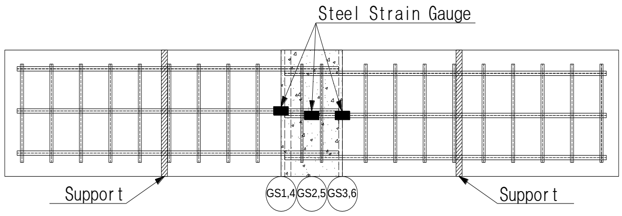

(c) Steel strain gauges (Plan)

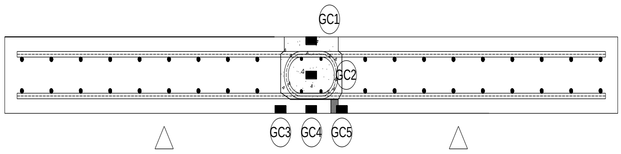

(d) Concrete strain gauges (Elevation)

Fig. 5 Measurement plan

behavior. For this purpose, measurements were performed by using a linear variable differential transformer (LVDT), six steel strain gauges, five concrete strain gauges, and two omega gauges for measuring the crack widths of each specimen. Fig. 5 illustrates the measurement scheme for the experimental program. An LVDT, as one of the electrical transformers for measuring deflections, was placed below the mid-span point where the maximum deflection occurred. For the measurement of crack width, two omega gauges were attached on the concrete surfaces, where the initial cracks occurred during the tests.

All of the specimens were supported as a simple beam, as shown in Fig. 6. The supports were located at a distance of 650 mm from each end, symmetrically. As illustrated in Fig. 6, a monotonic vertical load was applied to the mid-point of each specimen by a hydraulic actuator with capacity of 2000 kN and loading plate width of 200 mm.

The loading for all the tests was controlled according to the following procedure. After the stabilization of the applied load by repeated loading and unloading, reloading was followed by the load control method (0.5 kN/s) until an initial crack was observed. Then, the specimen was unloaded for installing two omega gauges on the surfaces where flexural cracks were observed near the bottom surface of mid-point. After attaching the omega gauges, loading was continued and the load control method was changed to the displacement control method (1 mm/min) until failure of the specimen. During the tests, the crack propagation on the surface of each specimen

Fig. 6 Test setup

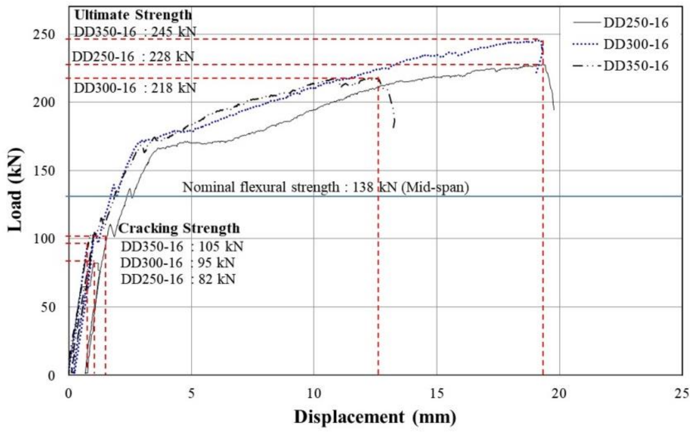

(a) DD-16 series

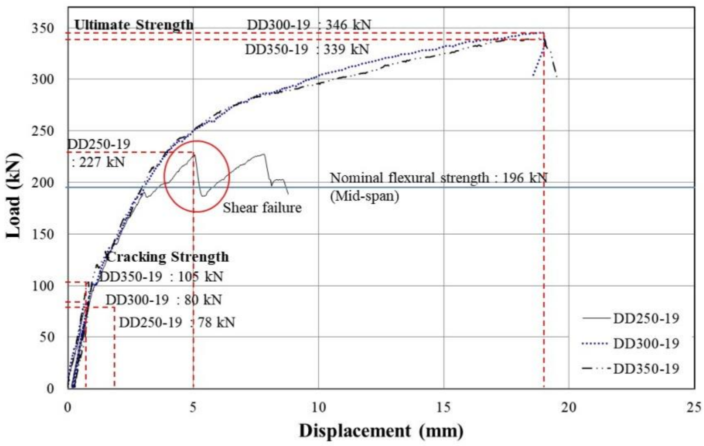

(b) DD-19 series

Fig. 7 Load–displacement curves based on joint spacing

was marked, and the displacement and strain data of reinforcement and concrete were recorded by using a data logger. In addition, the failure modes of the specimens were also thoroughly observed.

3. Test results and discussion

The structural behavior, including ultimate load capacity, failure mode, and crack formation and propagation, was investigated by the experimental program for loop joint details.

3.1 Load-displacement behavior

Fig. 7 presents the load–displacement curves that were plotted by using the measured displacements from an LVDT installed at the mid-point location of the specimen. The curves were sorted according to the widths of the joint and diameters of the loop bars. Moreover, the initial cracking loads and ultimate strengths were marked in the curves.

The load-displacement curves comprised three stages: linear, crack-propagation, and failure stages. In the first stage, the displacement increased linearly with the increase in the applied load. The curves showed non-linear behavior after an initial crack occurred. However, the curves seemed linear to some degree owing to the surplus elasticity of the reinforcement arranged in the specimen until it yields. The gradients of the curves decreased gradually and reached the yielding point. Lastly, ductile behavior was presented in the curves after yielding of the reinforcement.

The effect of the joint spacing on the ultimate strength was not significant. All the specimens showed considerable ductility and reasonable ultimate strength before failure, although the DD250-19 specimen showed inclined shear cracks and ruptured with an abrupt decline in loading during the ductile stage. Accordingly, the calculated nominal moments (Mn) of the specimens are greater than the ultimate moment capacity (Mu). Therefore, the allowable joint width of more than 250 mm can be used for the design of the specific joint detail.

Different diameters of reinforcement (16 mm, 19 mm) were used to investigate the behavior of the specimens based on the diameter of the loop bar. Prior to occurrence of the first crack, the load-displacement curves showed similar gradients regardless of the diameter of the loop bar. However, as the diameter of the loop bar was increased, the gradients of the load–displacement curves became steeper after cracking. According to Fig. 7, the larger diameter loop bar showed an increase of 41% in flexural strength of the beam (DD300 series). The specimens with the high strength filler in the joint did not show higher strength. Comparing the average strength of the specimens (DD300-22S, C, B) with normal strength filler, the flexural strength of the DD300-19 specimen was 5% lower than the specimens with high strength filler. Except the DD250-19 specimen, the displacement at failure of the specimens with high strength concrete showed better ductility than the specimens with normal concrete.

3.2 Flexural strengths

The designed specimens were intended to have a ductile failure. Through this, it was expected that the concrete in the compression zone would be crushed after reaching the yield strength of the reinforcement. Prior to the static tests, the flexural nominal strengths were calculated, in advance, by using the criteria of ACI 318 code (2014), and then the calculated strengths were compared with the test results. Table 4 presents the experimental and predicted ultimate flexural strengths and their comparisons. The ultimate strengths of the specimens with high strength filler were 70% higher than the calculated values, while the specimens with normal strength filler showed 40% higher strength. Accordingly, all the specimens showed sufficient flexural performance and the loop joint details used in the experimental program secured reasonable development lengths for

Table 4 Ultimate flexure strengths and failure modes

Specimen	Ultimate strength			Calculated shear strength (kN)	Failure mode
	Experiment (kN)	Calculated nominal flexural strength (kN)	Experiment/ Calculation		
DD250-16	228	138	1.65	122	Flexural
DD250-19	227	196	1.16	122	Flexure + Shear cracks
DD300-16	245	138	1.76	122	Flexural
DD300-19	346	196	1.77	122	Flexural
DD350-16	218	138	1.58	122	Flexural
DD350-19	339	196	1.73	122	Flexural
	Average		1.70	*DD250-19 was excluded*	
DD300-22S	361	260	1.39	244	Flexural
DD300-22C	390	260	1.50	244	Flexural
DD300-22B	343	260	1.32	244	Flexural
	Average		1.40		

Table 5 Cracking strengths and failure modes

Specimen	Cracking strength		
	Experiment (kN)	Calculation (kN)	Experiment/Calculation
DD250-16	82	47	1.74
DD250-19	78	47	1.66
DD300-16	95	50	1.90
DD300-19	80	50	1.60
DD350-16	105	53	1.98
DD350-19	105	53	1.98
DD300-22S	35	101	0.44
DD300-22C	Occurred before test	101	-
DD300-22B	Occurred before test	101	-

developing the required strengths. For the loop reinforcement to have sufficient development length, the specimen had twice the reinforcement in the joint parts than ordinary cast-in-place reinforced concrete beams.

3.3 Cracking and failure modes

Initial cracking loads were varied according to the width of the joint because the calculation of initial cracking strength was based on the location of the initial crack at the interface section. Thus, the cracking moment of each specimen is proportional to the distance measured from the mid-point to the interface.

Table 5 presents the cracking strengths and the calculated strength values. The cracking strengths in the experiments were derived based on the applied load value at the time of initial crack generation. For all the specimens, the initial cracks were observed near the interface section and cracks were generated under an applied load value between 75 kN and 95 kN. The cracking

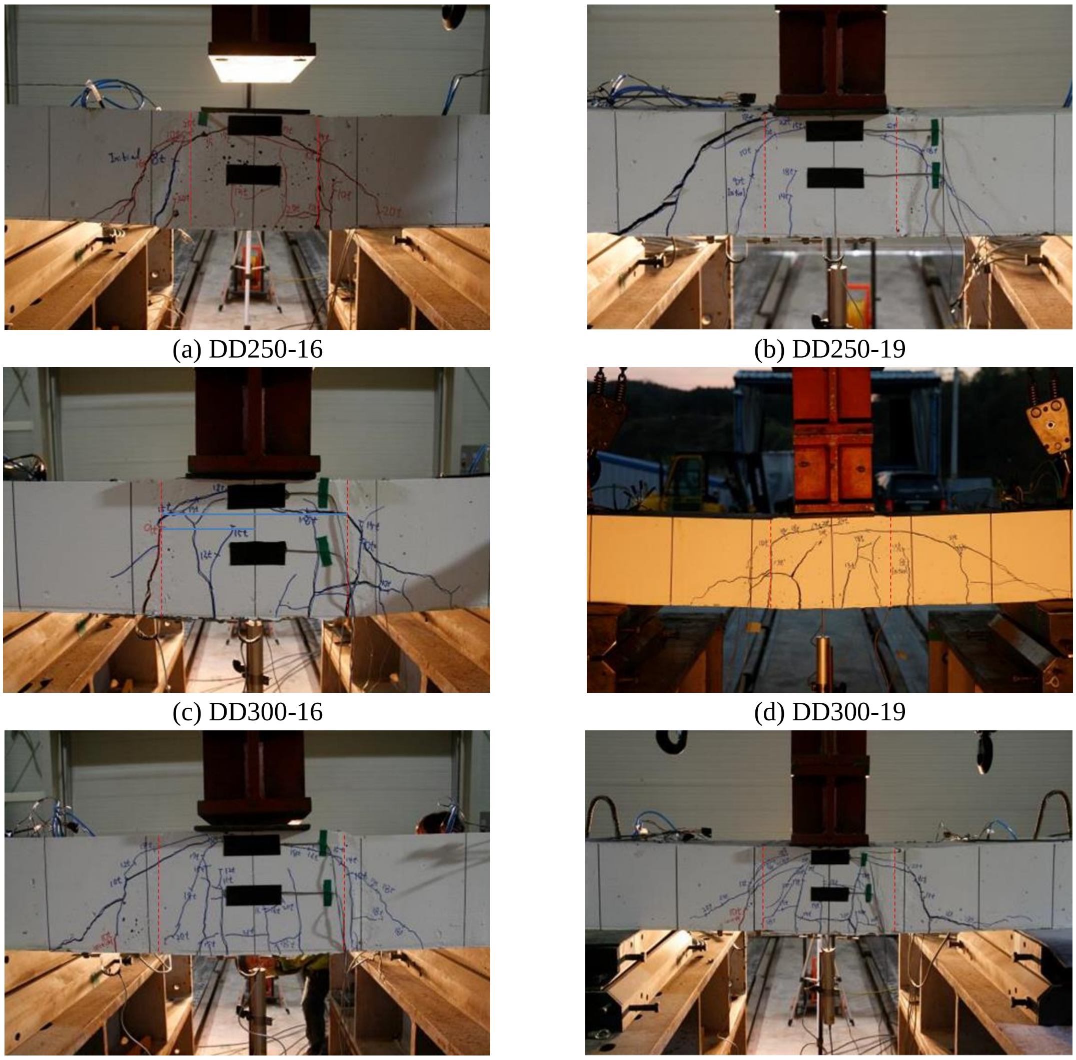

(a) DD250-16
(b) DD250-19
(c) DD300-16
(d) DD300-19
(e) DD350-16
(f) DD350-19

Fig. 8 Cracking patterns and failure modes (red dotted line as interface)

strength was approximately 1.8 times greater than the expected calculation value. The specimens with normal strength concrete in the joint showed initial cracks during the delivery and erection process. DD300-22S specimen showed a much lower cracking load value than the calculated value, while the high strength concrete showed significant enhancement in crack strength, as summarized in Table 5. The specimens with longer joint spacing showed a slight increase in cracking strength. It is recommended to use high strength filler and longer joint spacing for better quality control of the loop joint, while it is hard to prevent cracking of the loop connection with normal strength concrete at the joints after casting the concrete.

Fig. 8 presents the cracking patterns and final failure modes of each specimen. During the experiments, it was noticeably observed that initial cracking always occurred at the interface section, although the maximum moment was at the mid-point section. For each specimen, after the

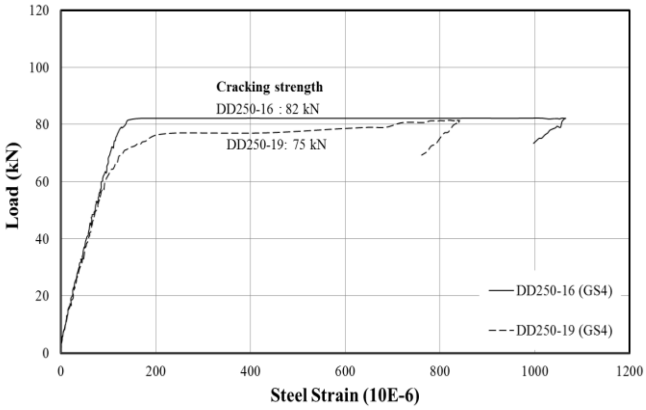

(a) DD250 series

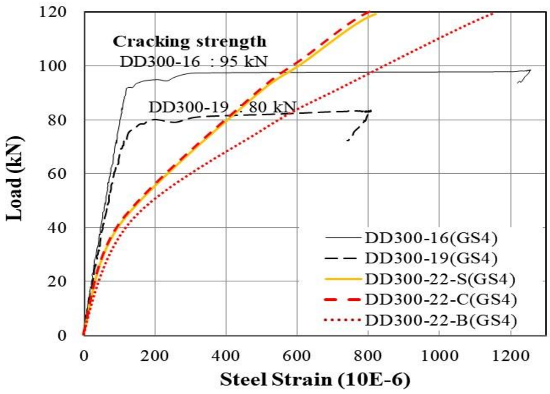

(b) DD300 series

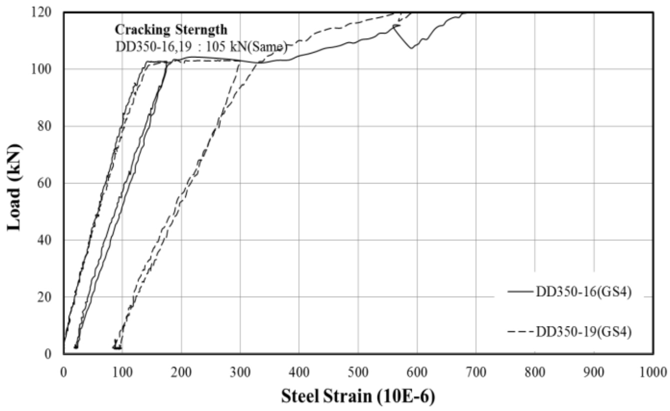

(c) DD350 series

Fig. 9 Steel-Strain curves according to diameter of loop reinforcements

generation of the initial cracks, vertical cracks propagated toward the respective end. Then, the distribution of the diagonal cracks in the compression zone was observed when the applied load nearly reached the ultimate load. By increasing the applied load value, the crack width also increased, leading to the failure of the specimen. All the specimens showed distributed cracking patterns without concentration of cracks at the two interface parts. Therefore, this phenomenon verified that the reinforcements in the concrete were well anchored and the development lengths of the reinforcement were sufficient for developing the strength.

In addition to direct observation of the initial cracks and identification of the cracking points by the load–displacement curves, the initial cracking points were confirmed through the steel-strain graphs of each specimen in Fig. 9. In each graph, the slopes of the specimens with high strength concrete were linear before cracking; however, the slopes became flat after cracking. Specimens with normal strength filler showed gradual increase in tensile stress of the reinforcement, as shown in Fig. 9(b). Moreover, the values of steel strain were extraordinarily higher, which means that the amount of the load taken by the reinforcement rapidly increased by the disruption of concrete accompanying the occurrence of the initial cracks. However, after the initial cracks occurred, the steel strains in the specimens with joint width of 350 mm increased relatively less than those in the other specimens. The stress in the specimens with 350 mm joints only reached 60 MPa, while the other specimens showed stress of around 200 MPa. The initial cracks at the joints and the flexural cracks at the mid-point of the specimens with 350 mm joint parts occurred approximately at the same time. Therefore, the use of 350 mm joint spacing is advisable to avoid stress concentration at the joints. This width also induces distribution of the flexural cracks at the time of initial crack generation by using high strength concrete as filling material of the loop joints.

As mentioned above, the experimental cracking strengths of the specimens with high strength concrete as filling material were drastically improved, up to approximately 200% in comparison to the theoretical values. Therefore, the use of high strength concrete in the joint parts showed an effect on the cracking strength, and it minimized the possibility of cracking of the joint.

3.4 Crack width calculation of the precast joint

In the joints of precast elements, cracks are unavoidable owing to weakness of the joint surface between the hardened precast concrete and the fresh filling material. The compressive stress of the joint by pre-stressing or imposed deformation can minimize this possibility. Otherwise, cracks should be controlled by the reinforcement and crack control measures to keep crack widths below acceptable limits. According to previous research results (Beeby 1978a, b), no direct relationship between corrosion and crack width exists and crack widths up to 0.4 mm do not significantly reduce the corrosion protection of the reinforcement in concrete. In order to confirm the current provision for crack control, it is necessary to estimate the crack width of the loop connection. The crack widths of the tested specimens using high strength concrete for the joint parts were evaluated to verify the performance of crack width control in the limit of serviceability.

The calculation of the crack width in Eurocode-2 is defined by multiplying the maximum crack spacing by the strain difference of the reinforcing steel and concrete, as in Eq. (1). If the spacing of the bonded reinforcement of the tensile zone is less than $5(c+\emptyset/2)$, the maximum crack spacing, $s_{r,\max}$, is calculated by Eq. (2). Crack spacing is a function of the concrete tensile strength, bond stress distribution, bar diameter, steel cross section, and effective concrete area in tension.

$$w_k = s_{r,max}(\varepsilon_{sm} - \varepsilon_{cm}) \tag{1}$$

$$s_{r,max} = k_3 c + k_1 k_2 k_4 \emptyset / \rho_{p,eff} \tag{2}$$

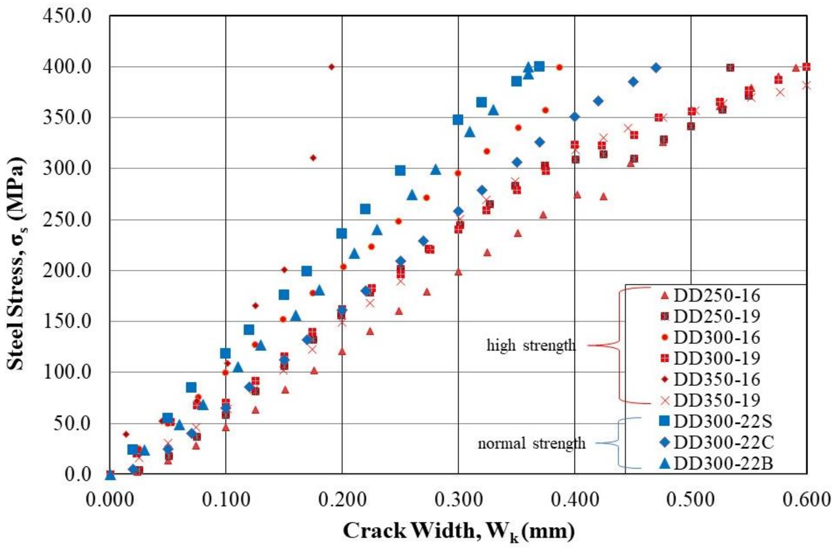

Fig. 10 Steel stress vs. crack width curves of test specimens

where, c is the cover of concrete and $\varnothing$ is the diameter of the reinforcement.

The strain difference is calculated as in Eq. (3), and the calculated value is defined to be at least 60% of the strain of steel.

$$\varepsilon_{sm} - \varepsilon_{cm} = \frac{\sigma_s - k_t \frac{f_{ct,eff}}{\rho_{p,eff}}(1 + \alpha_e \rho_{p,eff})}{E_s} \geq 0.6 \frac{\sigma_s}{E_s} \tag{3}$$

where k_t is a factor dependent on the duration of the loading and the $f_{ct,eff}$ variable is the mean value of the tensile strength of concrete, effective at the time when the first cracks may be expected to occur. The mean axial tensile strength, f_{ctm} is used as $f_{ct,eff}$. $\rho_{p.eff}$ is the ratio of steel to the effective tension area, $A_{c,eff}$. σ_s is the stress in the tension reinforcement, assuming a cracked section.

Fig. 10 presents the relationship between steel stress and crack width, which were measured at the crack location of the joint interface. The relation of the two variables was linear, as expected from the design provision. However, the specimens with high strength material at the joint showed greater crack width at the same steel stress than the specimen with normal strength material. Smaller reinforcement is more effective for crack width control than larger reinforcement. A few specimens showed a different trend because the cracks at the two interfaces of the connection were not symmetric.

There are special considerations in the crack width calculation. For evaluation of the strain difference term, the steel stress needs to be calculated at the location of the interface instead of at the location of maximum moment. From the observation of cracks as presented in Fig. 8, cracks are concentrated at the interfaces therefore cracks at the interfaces were greater than cracks at the center of the beam, even though the bending moment at the center ($M_{\max}$) is greater than the moment at the joints (M_j). The smaller strength between the precast element and joint filler is used as tensile strength. In the loop joint of the precast members, the maximum crack spacing, $s_{r,\max}$, can be assumed as the joint length when the length is bigger than the calculated spacing. This is

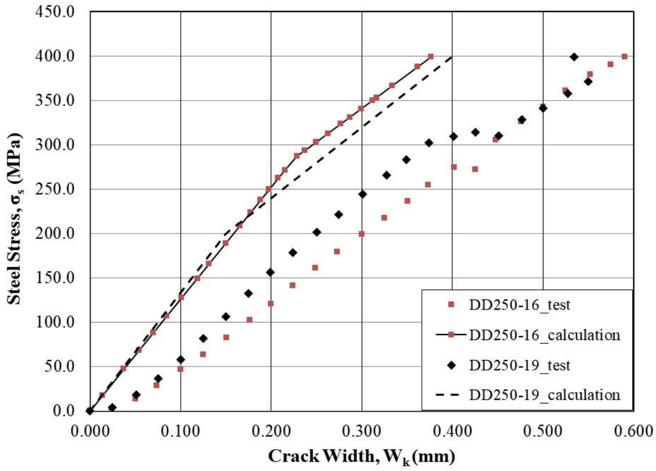

(a) DD250 specimens

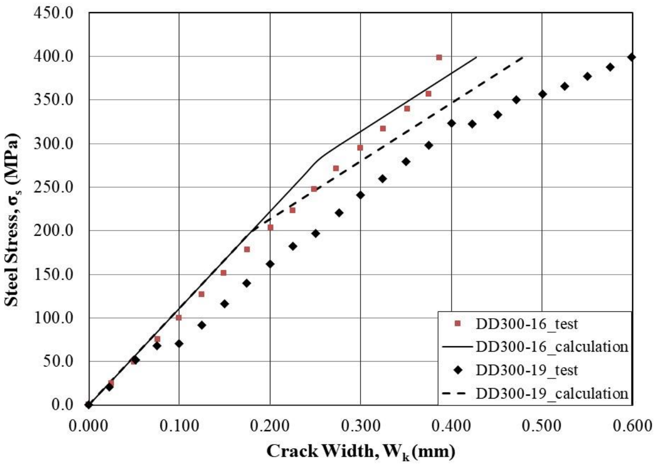

(b) DD300 specimens

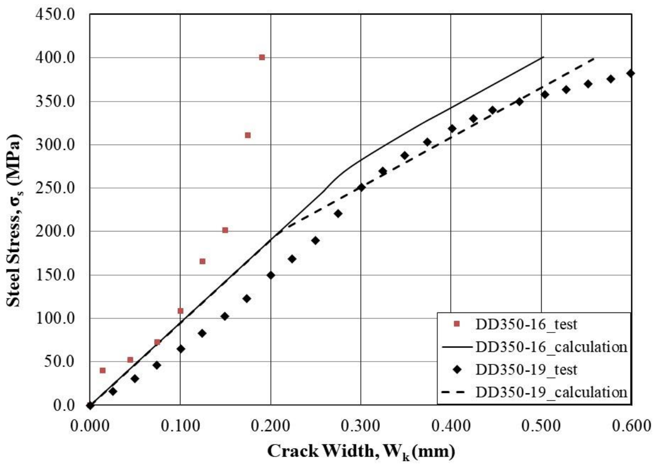

(c) DD350 specimens

Fig. 11 Comparisons of steel stress vs. crack width

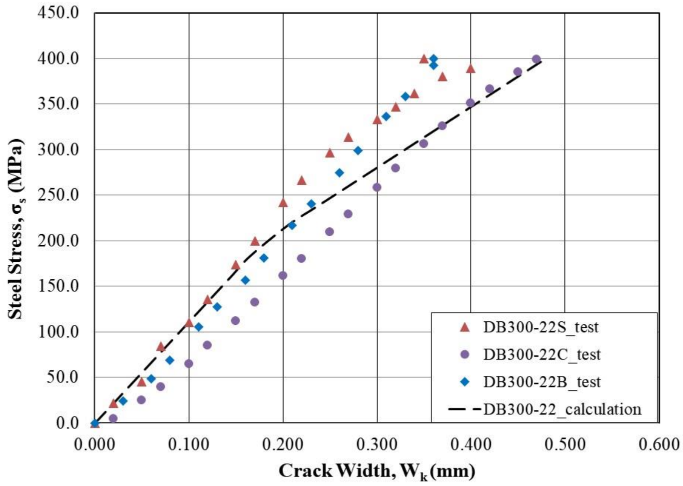

(d) DD300-22 specimens

Fig. 11 Continued

because the maximum crack width occurs at the interface, regardless of whether the initial crack occurs at the location of the maximum bending moment or at the location of the interface. Fig. 11 shows comparisons between the test results and the calculation based on these considerations. DD250-16 and DD250-19 specimens showed larger crack width than the calculated values, assuming the above considerations. It can be said that lap length of the loop is not enough to control the crack width for these two specimens, even though the loop joint provided greater flexural strength than the design value. DD300 and DD350 specimens, with high strength filler, showed better crack width control than the calculated characteristic crack width. The loop joint with normal strength concrete showed a non-conservative estimation, up to steel stress of around 200 MPa.

In the range of these experimental parameters, the current design provision for crack width calculation did not provide an appropriate evaluation. Even though the high strength concrete at the joint was better to control the initial cracks, the load for crack width of 0.2 mm, based on the current design codes, was showed only in 50% of the test results in the case of DD250 specimens. It was showed that the characteristic crack width of the loop joint with normal concrete had better prediction by the design codes. From these observations, it is necessary to modify the current design equations for crack width considering the cracking behavior of the loop joints of precast members.

4. Conclusions

Loop joints are widely used for the connection details of precast decks. For practical purposes, there were many attempts to reduce the length of the joint using high strength material. This experimental study was performed to investigate the validity of the current design codes for crack width calculation for the loop joint with reasonable assumptions. From the experimental study, it is concluded that:

- All the specimens showed considerable ductility and reasonable ultimate strength when the length of the loop joint was more than 250 mm, which is based on the current design requirement of the details. The ultimate strength of the specimens with high strength filler was 70% higher than the calculated values, while the specimens with normal strength filler showed 40% higher strength.
- The use of high strength concrete in the joint parts showed better performance in terms of cracking load. The high strength filler at the joints is favorable to minimize the possibility of cracking of the joint. Specimens with longer joint spacing showed a slight increase in cracking strength. It is recommended to use a high strength filler and longer joint spacing for better quality control of the loop joint, while it is hard to prevent cracking of the loop connection with normal strength concrete at the joints after casting concrete.
- In the range of these experimental parameters, the current design provisions for crack width calculation for the loop joint did not provide an appropriate evaluation. The loop joints with longer joint spacing and normal concrete showed less difference in cracking load of 0.2 mm width from the calculated values. From this observation, the current design equations on crack width cannot be used to evaluate the crack width of the loop joint for precast members.

It is necessary to have more data to propose a modified crack width calculation for loop joints of precast elements. The use of high performance concrete for the loop joint to minimize the joint spacing should carefully consider the crack width control when the service loads produce higher tensile stress at the joint than the cracking strength of the interface.

References

AASHTO LRFD (2013), AASHTO LRFD Bridge Design Specifications, American Association of State Highway and Transportation Officials, Washington, D.C.

ACI 224.3R (2005), Joints in Concrete Construction, American Concrete Institute, Farmington Hills, MI.

ACI 318-14 (2014), Building Code Requirements for Structural Concrete and Commentary and Notes, American Concrete Institute, ACI Committee 318, Detroit.

Beeby, A.W. (1978), “Corrosion of reinforcing steel in concrete and its relation to cracking”, *Struct. Eng.*, **56A**(3), 77-81.

Beeby, A.W. (1978), “Cracking: what are crack width limits for?”, *Concrete*, 31-33.

Creazza, G. and Russo, S. (1999), “A new model for predicting crack width with different percentages of reinforcement and concrete strength classes”, *Mater. Struct.*, **32**, 520-524.

EN 1992-1-1 (2005), Eurocode 2-Design of concrete structures-Part 1-1: General Rules and Rules for Buildings, European Committee for Standardization.

Hanswille, G. (1986), “Zur Ribreitenbeschränkung bei Verbundträgern”, *Techn.-Wiss. Mitteilung*, **86-1**, Institut für Konstruktiven Ingenieurbau, Ruhr-Universität Bochum.

Issa, M.A., Khayyat, S.Y., Yousif, A.A. and Kaspar, I.I. (1995), “Field performance of full depth precast concrete panels in bridge deck reconstruction”, **40**(3), 82-108.

Issa, M.A., Yousif, A.A., Issa, M.A. Kaspar, I.I. and Khayyat, S.Y. (1998), “Analysis of full depth precast concrete deck panels”, *PCI J.*, **43**(1), 74-85.

Joergensen, H.B. and Hoang, L.C. (2015), “Strength of loop connections between precast bridge decks loaded in combined tension and bending”, *Struct. Eng. Int.*, **25**(1), 71-80.

Lewis, S. (2009), “Experimental investigation of precast bridge deck joints with U-bar and headed bar joint details”, University of Tennessee, Knoxville.

LSD Bridge Design (2012), “Limit state based bridge design specification”, Korea Road and Transportation Association.

Perry and Royce (2007), "Innovative field-cast UHPC joints for precast bridge decks (side-by-side Deck Bulb-Tees)", Village of Lyons, NY-Design, Prototyping, Testing and Construction.
Rosenthal, I. and Shimoni, J. (1984), "Bending behaviour of a double-loop connection between precast concrete slabs", *Concrete Int.*, **11**, 30-34.
Ryu, H.K., Chang, S.P., Kim, Y.J. and Kim, B.S. (2005), "Crack control of a steel and concrete composite plate girder with prefabricated slabs under hogging moments", *Eng. Struct.*, **27**, 1613-1624.
Ryu, H.K., Kim, Y.J. and Chang, S.P. (2007), "Crack control of a continuous composite two-girder bridge with prefabricated slabs under static and fatigue loads", *Eng. Struct.*, **29**, 851-864.
Ryu, H.K., Kim, Y.J. and Chang, S.P. (2007), "Experimental study on static and fatigue strength of loop joints", *Eng. Struct.*, **29**(2), 145-162.
Shim, C.S., Chung, C.H., Kim, I.K. and Kim, Y.J. (2010), "Development and application of precast decks for composite bridges", *Struct. Eng. Int.*, **20**(2), 126-133.
Shim, C.S., Kim, J.H., Chung, C.H. and Chang, S.P. (2000), "The behaviour of shear connections in composite beam with full-depth precast slab", *Proc. Inst. Civil Eng. Struct. Build.*, **140**, 101-110.
Shin, D.H., Chung, C.H., Oh, H.C., Park, S.J., Kim, I.G., Kim, Y.J., Byun, T.K. and Kang, M.G. (2016), "Structural behaviour of precast concrete deck with ribbed loop joints in a composite bridge", *Smart Struct. Syst.*, **17**(4), 559-576.
Vitek, J.L., Citek, D., Kolisko, J., Coufal, R. and Jursik, P. (2016), "Application of UHPC joints in precast structures", *Solid State Phenomena*, **249**, 267-272

CC